Separation Science and Technology
Publication details, including instructions for authors and subscription information:
http://www.informaworld.com/smpp/title~content=t713708471

Vacuum Sorption Pumping Studies of Argon and Oxygen on 4A Molecular Sieves

J. J. Perona[a]; C. H. Byers[a]; J. K. Prazniak[b]
[a] Chemical Technology Division, Oak Ridge National Laboratory, Oak Ridge, Tennessee [b] Oak Ridge Y-12 Plant, Martin Marietta Energy Systems, Oak Ridge, Tennessee

To cite this Article Perona, J. J. , Byers, C. H. and Prazniak, J. K.(1993) 'Vacuum Sorption Pumping Studies of Argon and Oxygen on 4A Molecular Sieves', Separation Science and Technology, 28: 1, 595 — 614
To link to this Article: DOI: 10.1080/01496399308019509
URL: http://dx.doi.org/10.1080/01496399308019509

SEPARATION SCIENCE AND TECHNOLOGY, 28(1-3), pp. 595-614 (1993)

VACUUM SORPTION PUMPING STUDIES OF ARGON AND OXYGEN ON 4A MOLECULAR SIEVES*

J. J. Perona† and C. H. Byers
Chemical Technology Division
Oak Ridge National Laboratory
Oak Ridge, Tennessee 37831

J. K. Prazniak
Oak Ridge Y-12 Plant
Martin Marietta Energy Systems
Oak Ridge, Tennessee 37831-8001

ABSTRACT

Cryosorption pumping is a method of evacuating enclosed volumes by adsorbing gas on a deep bed of sorbent, such as Davison 4A zeolite, at cryogenic temperatures. Modeling the dynamic behavior of these systems for air pumping requires information on two major constituents of air: oxygen and argon. Particle size variation was the major variable in determining the mechanism of the process. The model comprises a fluid-phase mass balance representing the dynamics of gas in the bed and a spherical, one-dimensional diffusion equation describing adsorption in pellets of 4A zeolite. The present model calculates effective pore diffusivity taking into account Knudsen diffusion, ordinary diffusion, and Poiseuille flow. The primary diffusional resistance appears to occur in the macropores formed by the pelletizing clay binder, rather than in the bed interstices or microporous zeolite crystals.

---

*Research sponsored by the Division of Chemical Sciences, Office of Basic Energy Sciences, U.S. Department of Energy under contract DE-AC05-84OR21400 with Martin Marietta Energy Systems, Inc.

†Author to whom correspondence is to be addressed.

INTRODUCTION

Cryosorption pumping is a method of evacuating an enclosure by adsorbing the contained gases on a refrigerated solid sorbent. It is currently used in a number of instrumentation applications and holds promise for evacuating large chambers associated with advanced energy applications. Investigators have typically studied the sorption behavior of air at temperatures from 77 to 100 K, but new applications have emphasized the sorption of individual gases as well. Helium and hydrogen are of current interest in the study of fusion reactors, where large volumes of those gases must be removed from magnetic and radioactive environments. Experiments to study the cryopumping of hydrogen and helium have been carried out at temperatures as low as 4.2 K (1).

Cryosorption pumps have also been employed to remove argon used in the sputter coating of semiconductor devices (2). Such pumps can also be used to adsorb and hold hazardous gases from remote areas temporarily until a disposition can be determined (3).

Typically, cryosorption pumping is performed in a fixed bed of molecular sieves in which all the sorbate that enters the bed is adsorbed and no flow exits the bed. Figure 1 shows the basic components of the sorption pumping experiment in a simplified manner. Depending on the experiment, either liquid nitrogen or an acetone-dry ice bath is used to control the temperature of the bed. The experiment simply consists of allowing a constant flow of a gas to be admitted to a previously evacuated and desorbed bed of molecular sieves. The pressure in the gas phase above the bed and at several locations down the bed is measured as the run progresses. The pressure range of interest is below 1 torr (133 Pa) for the vacuum applications of interest, so tests are terminated when the above-bed pressure reaches that range.

Various sorbents may be used in cryopumping applications, but zeolite molecular sieves are preferred because of their high pumping speed, physical stability, and chemical inertness. An aspect of cryosorption pumps that has not been thoroughly studied is the fundamental transport phenomena

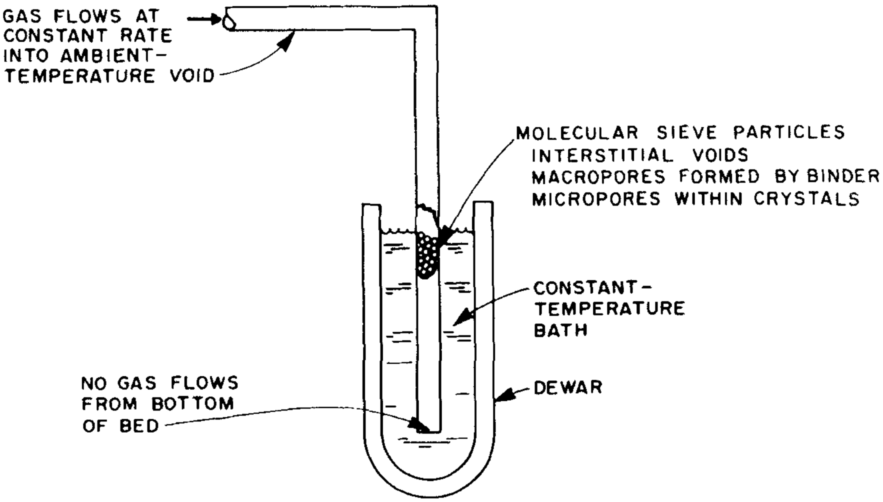

FIGURE 1. Primary components of an experimental apparatus for observing the cryosorption behavior of gases.

which underlie cryopumps. In a previous series of experiments, Crabb and Perona(4) began studing the individual components of air using nitrogen and carbon dioxide as their sorbed gases. The purpose of this study is to observe the sorption behavior of the two remaining major components of air: argon and oxygen, in fixed beds containing the same type of 4A molecular sieve as was used by the previous experimenters and to compare the results with the model of Prazniak and Byers (5).

EXPERIMENTAL

In their experiments, Crabb et al. (6) used the apparatus shown in Fig. 2 to adsorb N_2 and CO_2 on zeolite 4A molecular sieve. Pressurized gas flows from a cylinder through a calibrated stainless steel orifice. The gas leak rate is determined by the back pressure on the system. The leak rates of argon and oxygen were 3.68 x 10^{-9} and 4.09 x 10^{-9} mol/s, respectively.

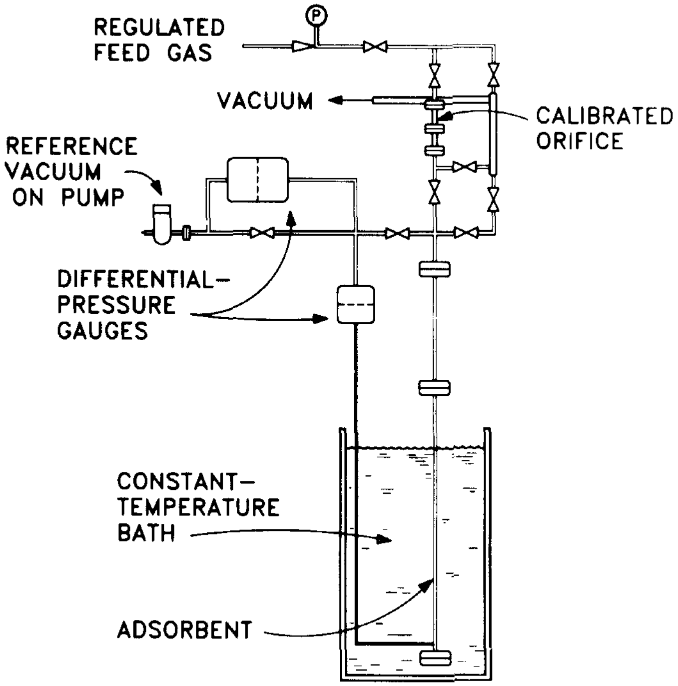

FIGURE 2. Detailed schematic diagram of the sorption pumping apparatus used in the current study.

The bed is a 20-cm section of 0.77-cm-ID stainless steel tubing. Differential pressure cells were connected to the top and bottom of the bed with 0.63-cm-OD tubing. The millivolt signal from the capacitance manometers was converted to a digital signal by an A/D conversion board (Data Translation Model 2801) interfaced to a microcomputer (IBM PC-AT) for graphical display and digital data storage. A computer code was used to convert these signals to absolute pressure and to monitor the pressure at preset time intervals throughout the run. Throughout the runs a reference of $\sim 10^{-3}$ torr (0.133 Pa) was maintained with an ion pump.

The sorbent was from the same batch of 4A synthetic zeolite molecular sieve (Davison Chemical Division of W. R. Grace and Company) as was used by Crabb et al. (6). The material is nominally spherical, with a size range of 0.42 to 1.41 mm (40 to 14 mesh). The pellets were sized into fractions using wire mesh screens. Two series of runs were made, one with diameters ranging from 0.50 to 0.60 mm (35 to 30 mesh) and the other from 0.35 to 0.42 mm (45 to 40 mesh). In the earlier study it was determined that the mean-crystal size of the zeolite was ~1.85 μm and that there was a considerable range around this mean.

Before a run, the bed was held at 200°C for 2 h while it was evacuated using an external pumping system. The bed was cooled to room temperature, isolated from the external pump, and then submerged in the coolant (liquid nitrogen in the current series). After the pressure steadied to $\sim 10^{-3}$ torr and the bed had been allowed to stand in the coolant for 2 h, the valve from the gas cylinder was opened and data acquisition begun. Data were gathered from the experiment until the bed became saturated or a pressure of 1 torr was reached. Regeneration of the bed followed.

THEORETICAL BACKGROUND

The theoretical mass transport theory that describes the behavior of gases during sorption on zeolites under conditions of high vacuum was developed by Crabb et al. (6) and by Prazniak and Byers (5). The main challenge in modeling the system surrounds the nature of the mass transfer resistance of the 4A zeolite pellets, which consist of cubic crystals, with a mean-edge length of 1.7 to 2.0 mm, fixed in an inert binder. For the purposes of analysis, they were assumed to be spherical with volumes equal to the cube volumes. About 10% of the sieve-pellet volume is occupied by the binder, which includes some voids within the binder (macrovoids). The movement of molecular species within the crystals presumably occurs in the intracrystal voids (microvoids).

The remaining bed volume consists of interstitial voids between the pellets, which is usually referred to simply as the void fraction (ϵ). If the major transport resistance occurs within the macrovoids, as might be the case when crystal-surface adsorption occurs, a macropore model is used, and the characteristic size is the diameter of the molecular-sieve pellet. On the other hand, if the major resistance to transport is within the crystals, a micropore model is called for, and the characteristic size is the zeolite crystal equivalent diameter. The characteristic lengths in these two limits are an order-of-magnitude different.

The unsteady-state mass balance on a differential section of bed is a typical one for granular bed applications:

$$\epsilon\frac{\partial c}{\partial t}+\epsilon\frac{\partial(vc)}{\partial z}+\rho_b\frac{\partial\bar{q}}{\partial t}=0\,. \tag{1}$$

The accumulation of sorbate within the volume in the fluid phase, $\epsilon\frac{\partial c}{\partial t}$, is related to the accumulation of material in the unit volume due to the changing flux of gas molecules through the interstices and macrovoids, $\epsilon\frac{\partial(vc)}{\partial z}$, and the mean accumulation of sorbate in the solid phase, $\rho_b\frac{\partial\bar{q}}{\partial t}$. The unsteady-state diffusion equation for a sphere in one dimension represents transient diffusion in the solid phase,

$$\frac{\partial q}{\partial t}=\frac{1}{r^2}\frac{\partial}{\partial r}\left[r^2 D_z\frac{\partial q}{\partial r}\right], \tag{2}$$

where D_z is the effective zeolitic diffusivity.

The boundary condition at the top of the bed ($z=0$) is given as a fluid-phase balance. This flux is expressed in terms of flow into the system and the accumulation of gas in the head space,

$$\epsilon AD_p\left.\frac{\partial c}{\partial z}\right|_{z=0}=\frac{Q}{RT_a}-\left.\frac{\partial c}{\partial t}\right|_{hs}, \tag{3}$$

where Q is the constant feed rate. The zero-flux condition at the bottom of the bed ($z=\ell$) is expressed as

$$\left.\frac{\partial c}{\partial z}\right|_{z=\ell}=0. \tag{4}$$

For the solid phase, a symmetry condition is implicit in the model, while solid-gas equilibrium is assumed at the sorbent-solid surfaces. In the pressure range of this study, concentration is related to pressure by the ideal gas law. The Langmuir isotherm,

$$\frac{q(R)}{q_m} = \frac{kp}{1+kp}, \tag{5}$$

was used by Crabb and Perona (4) to represent the adsorption of CO_2 and N_2 on zeolite 4A molecular sieve and is used in the current study for O_2 and Ar. Experimental isotherm data were available for pressures as low as 1 torr, but extrapolations were necessary to include the pressure range of the experiments.

The second term in Eq. (1), representing the flux of gas molecules through a cross section of the bed, can be represented using a form of Fick's law with an effective pore diffusivity, D_p:

$$\frac{\partial(vc)}{\partial z} = D_p \frac{\partial^2 c}{\partial z^2} \,. \tag{6}$$

The pore diffusion has three significant contributions in the vacuum sorption case: D_K, the Knudsen diffusion, D_m, the molecular diffusion; and, D_{Pois}, the Poiseuille diffusion. Ruthven (7) gives the following equation for estimating the effective pore diffusivity from the component diffusivities described above:

$$D_p = \left[\frac{1}{\frac{1}{D_K} + \frac{1}{D_m}}\right] + D_{\mathrm{Pois}} \,. \tag{7}$$

Ruthven (7) suggests the following equation for estimating D_K, the Knudsen diffusivity:

$$D_K = 9700\, r_p \left(\frac{T}{M}\right)^{0.5} , \tag{8}$$

where r_p is the mean-pore radius (cm), and M is the molecular weight of the diffusing species.

The molecular diffusivity can be estimated from the Chapman-Enskog equation (8), modified for a diffusing species that is an ideal gas:

$$D_m = 0.001858 \frac{\sqrt{\frac{2T^3}{M}}}{p\sigma^2\Omega} , \tag{9}$$

where σ and Ω are Lennard-Jones parameters. Ruthven (7) gave the following equation for estimating the contribution of Poiseuille flow to the gas diffusivity:

$$D_{\text{Pois}} = \frac{pr_p^2}{8\mu}, \tag{10}$$

where μ is the gas viscosity (g cm/s), which can be calculated from

$$\mu = 2.6693 \times 10^{-5} \frac{\sqrt{M \cdot T}}{\sigma^2 \Omega}. \tag{11}$$

Eq. (11) is from Bird, Stewart, and Lightfoot (8). For a system involving a gas in which the temperature is constant, Eqs. (8) and (10) reduce to functions of the pore radius, r_p, and the gas pressure, p.

At low pressures and small pore radii, the primary resistance to flow is collision of molecules with the pore walls. In this case Knudsen diffusion is dominant. At higher pressures, when collisions between molecules become the primary resistance to flow, molecular diffusion and Poiseuille flow are dominant. In the transition region, contributions from all three mechanisms may be computed using Eq. (7).

In the solid phase, the diffusivity of the sorbate within the crystals is also considered to be dependent on the concentration of the diffusing species. Garg and Ruthven (9) showed that the Darken equation can be used, which leads to the following relationship:

$$D_z = D_0 \left[\frac{\partial(\ln p)}{\partial(\ln q)}\right], \tag{12}$$

where D_z is the concentration-dependent, solid-phase diffusion coefficient and D_0 is the corrected diffusivity, which is a constant. Incorporating the concentration-dependent diffusivity, the diffusion equation for the sorbent particle can be rewritten as

$$\frac{\partial q}{\partial t} = \frac{1}{r^2}\frac{\partial}{\partial r}\left[r^2 D_z \frac{\partial q}{\partial r}\right]. \tag{13}$$

Returning to Eq. (1), it is not possible to express the average accumulation of the sorbate in the solid phase, $\rho_b \frac{\partial \bar{q}}{\partial t}$, as a simple function of the pressure.

However, it can be expressed in terms of the other dependent variable, the point solid loading, q. The concentration profile can be integrated to obtain $\bar{q}$, and $\partial\bar{q}/\partial t$ can be computed by difference, but it is numerically complex to do so. Instead, $\partial\bar{q}/\partial t$ can be calculated in terms of the sorbate flux at the surface of the crystal. Because the net flux in a crystal is inward, a crystal acts as a mass sink, and the flux of sorbate across the crystal surface is equivalent to the instantaneous mean accumulation in the crystal. The accumulation can be calculated from the concentration gradient at the crystal surface and the packing characteristics of the sorbent:

$$\frac{\partial\bar{q}}{\partial t} = D_z(q)\phi_z \left.\frac{\partial q}{\partial r}\right|_{r=R}, \tag{14}$$

where ϕ_z is the crystal-surface area per unit crystal volume, or $3/R$.

Incorporation of Eqs. (7) and (14) into the model Eqs. (1) and (2) yields the fluid balances in terms of the gas pressure and the solid loading:

$$\left.\frac{\partial p}{\partial z}\right|_z = \frac{RT}{\epsilon}\left\{\frac{\epsilon D_p(p)}{RT}\frac{\partial^2 p}{\partial z^2} - \left[D_z(q)\phi_z \left.\frac{\partial q}{\partial r}\right|_{r=R}\right]\right\}. \tag{15}$$

This balance with the previously stated boundary conditions represents a nonlinear system of equations, which must be solved numerically for realistic experimental situations. Prazniak and Byers (5) have applied orthogonal collocation methods to the solution. Four constants must be evaluated either by independent experiment or by some other means, such as theoretical computation or fitting parameters. Two of the parameters, k and q_m, are, respectively, the linear constant and the capacity factor in the Langmuir equilibrium equation. The single variable associated with the fluid-phase transport is r_p, the mean-pore radius of the interstitial or macrovoid volume. Finally, the solid-phase diffusion is characterized by D_0.

RESULTS AND DISCUSSION

The objective of this study was to further understanding of the sorption of the components of air, which was begun by Crabb and Perona (4), by reporting data on the cryosorption of O_2 and argon on 4A molecular sieves.

Sorption pumping experiments were done with argon at a flow rate of 6.88 x 10^{-5} torr L/s and oxygen at a flow rate of 7.65 x 10^{-5} torr L/s. Two beds of pellets were used for these experiments. The first bed, with an average pellet diameter of 0.55 mm (30–35 mesh) weighed 4.29 g. The second bed, with an average pellet diameter of 0.385 mm (40- -45 mesh), weighed 4.48 g. As shown by the experimental results in Figs. 3-6, saturation times were much less for argon than for oxygen. For the bed of larger pellets, saturation was approached in ~5 h for argon and 50 h for oxygen, even though the oxygen flow rate was larger. Similarly, for the bed of smaller pellets, saturation was approached in ~8 h for argon and 110 h for oxygen.

For both gases, the pellet size strongly affects the kinetics of adsorption. This is clear evidence that transport in the pellets is controlled by macropore diffusion rather than by micropore diffusion, since crystal-size distributions should be the same for all pellets. Extrapolation of measured diffusivities reported in the literature for argon and oxygen in 4A crystals tends to support control by macropore diffusion, because diffusivities in the crystals at 77 K are so small that very little diffusion can occur in other than the surface layers of the crystals within the time frame of the experiments.

Ruthven and Derrah (10) measured micropore diffusivities for these gases in 4A crystals in the temperature range of 200 to 330 K. Extrapolating their results to 77 K yields estimates for diffusivity in the neighborhood of 10^{-23} cm^2/s for argon and 10^{-19} cm^2/s for oxygen. Corresponding Fourier numbers ($D_0 t/s^2$) based on these extrapolated diffusivities and experimental run times are in the range of 10^{-6} for oxygen and 10^{-11} for argon. The ratio of mass adsorbed to capacity is of the order of the square root of the Fourier number. Thus, the penetration of the gases into the crystals is estimated to be extremely small.

The amounts of gases adsorbed in the experiments as saturation is approached were quite small. Values are presented in Table 1, calculated with constant influx rates of 4.09 x 10^{-9} mol/s for oxygen and 3.68 x 10^{-9} mol/s for argon. These saturation loadings range from 2.2 x 10^{-5} mol/g for argon on 0.55-mm pellets to 3.8 x 10^{-4} mol/g for oxygen on 0.385-mm pellets.

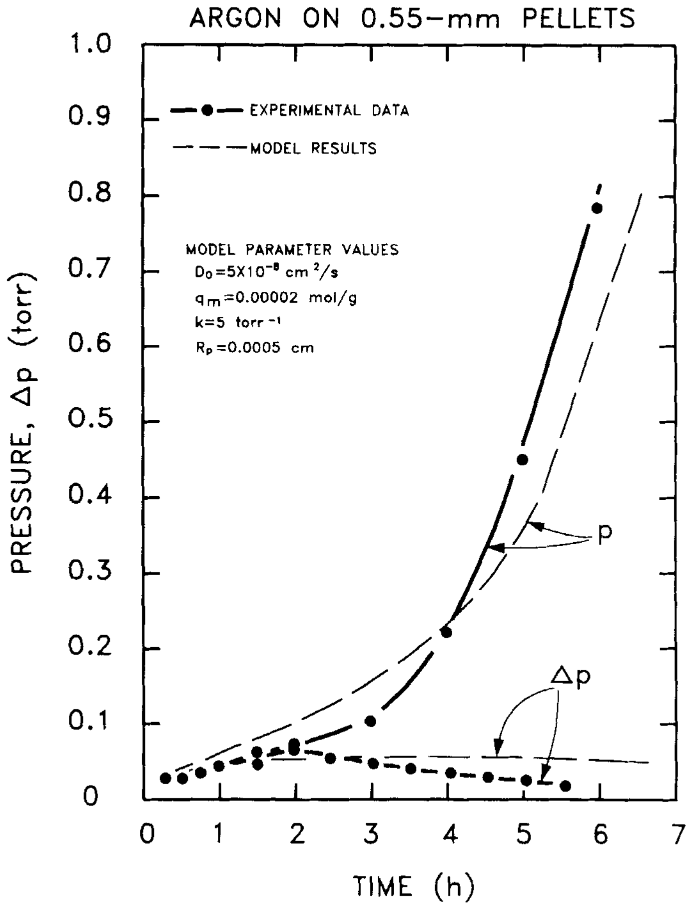

FIGURE 3. Comparison of experimental sorption pumping data for argon on 0.55-mm spherical pellets of Davison 4A zeolite molecular sieves with the results of the proposed macropore-controlled model.

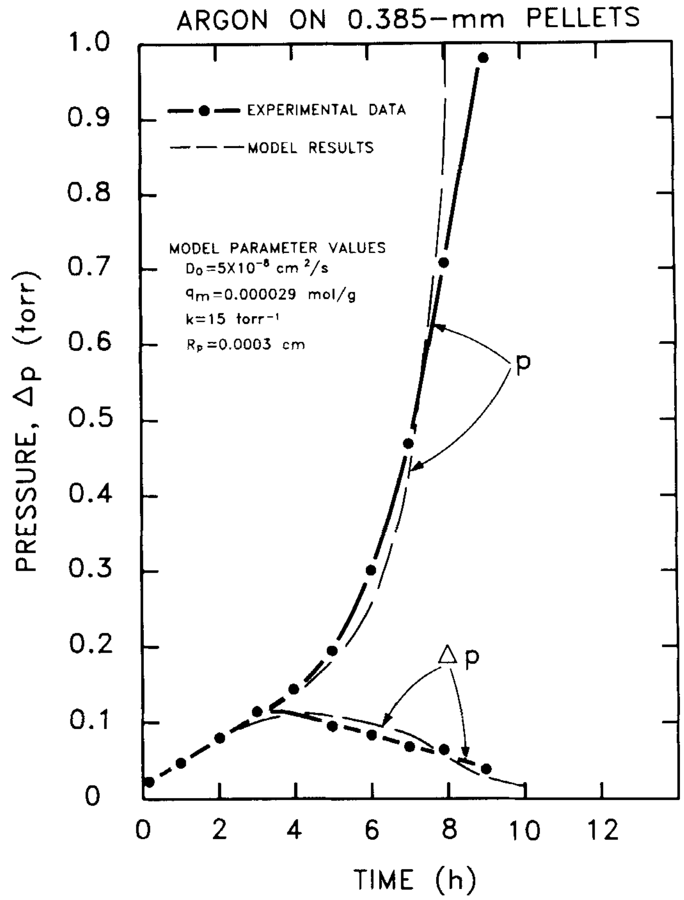

FIGURE 4. Comparison of experimental sorption pumping data for argon on 0.385-mm spherical pellets of Davison 4A zeolite molecular sieves with the results of the proposed macropore-controlled model.

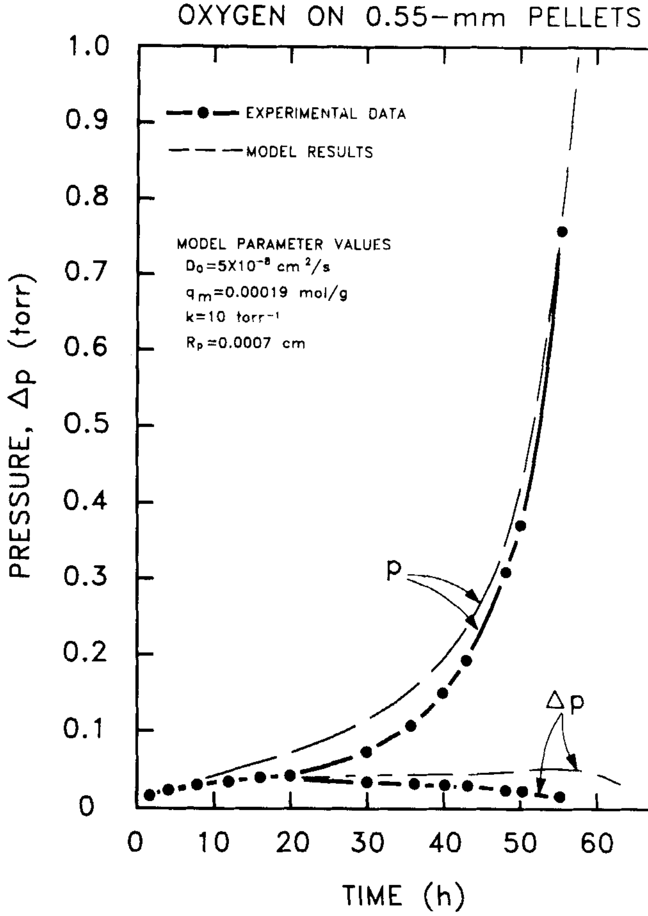

FIGURE 5. Comparison of experimental sorption pumping data for oxygen on 0.385-mm spherical pellets of Davison 4A zeolite molecular sieves with the results of the proposed macropore-controlled model.

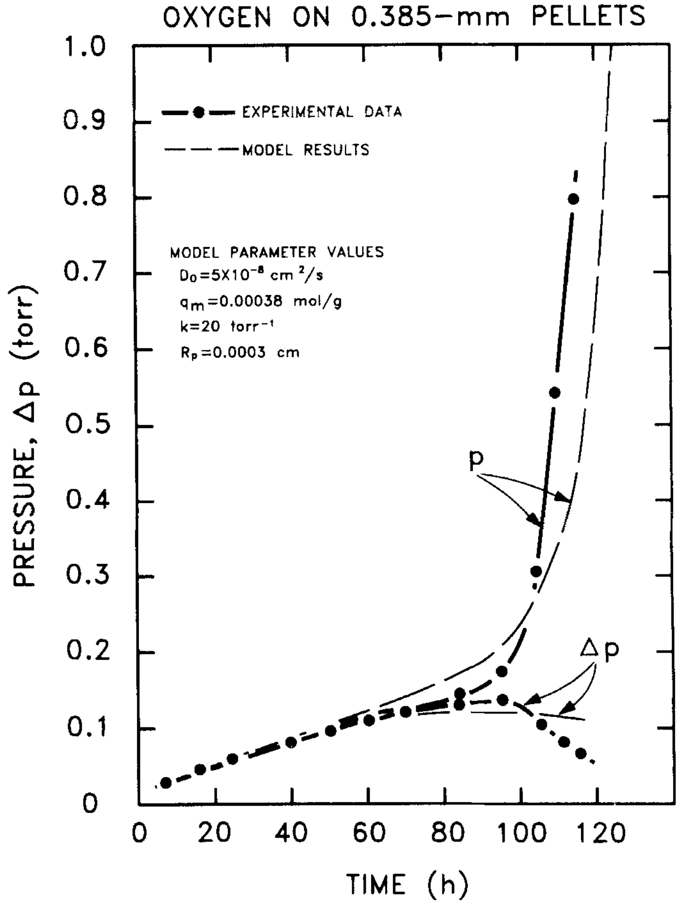

FIGURE 6. Comparison of experimental sorption pumping data for oxygen on 0.55-mm spherical pellets of Davison 4A zeolite molecular sieves with the results of the proposed macropore-controlled model.

Table 1. GAS LOADINGS AT SATURATION

	Argon		Oxygen	
	0.385 mm	0.55 mm	0.385 mm	0.55 mm
Time to saturation (h)	9	7	117	57
Gas absorbed (mol/g)	2.6×10^{-5}	2.2×10^{-5}	3.8×10^{-4}	2×10^{-4}

Ruthven and Derrah (11) report Henry's constants for these gases on 4A zeolites over a temperature range of 200 to 450 K. Using their values for heats of sorption in the van't Hoff equation, the amounts absorbed at 77K should be more than 10^6 times larger than at 273 K. This extrapolation would indicate equilibrium loadings of the order of 1 or 2 mol/g for argon and oxygen at 77 K.

Another way of evaluating the loadings in our experiments without making such large extrapolations with Ruthven and Derrah's data is to calculate the temperatures at which our observed loadings would be expected. These calculations yield 160 K for argon and 120 K for oxygen. These scoping calculations show clearly that saturation of the zeolite crystals was not approached in our pumping experiments at 77 K as the beds exhibited breakthrough.

In fitting our calculational model to the data in Figs. 3 through 6, the gas loadings in Table 1 were used as approximations for q_m. Only small adjustments to these values were required to achieve best agreement.

Ruthven and Derrah (1972) reported macropore diffusivity measurements for light hydrocarbon gases. Their values for effective diffusivities were of the order of 10^{-5}cm^2/s at temperatures in the range of 323 to 448K. Values of the order of 10^{-8}cm^2/s worked well in our model for the present results.

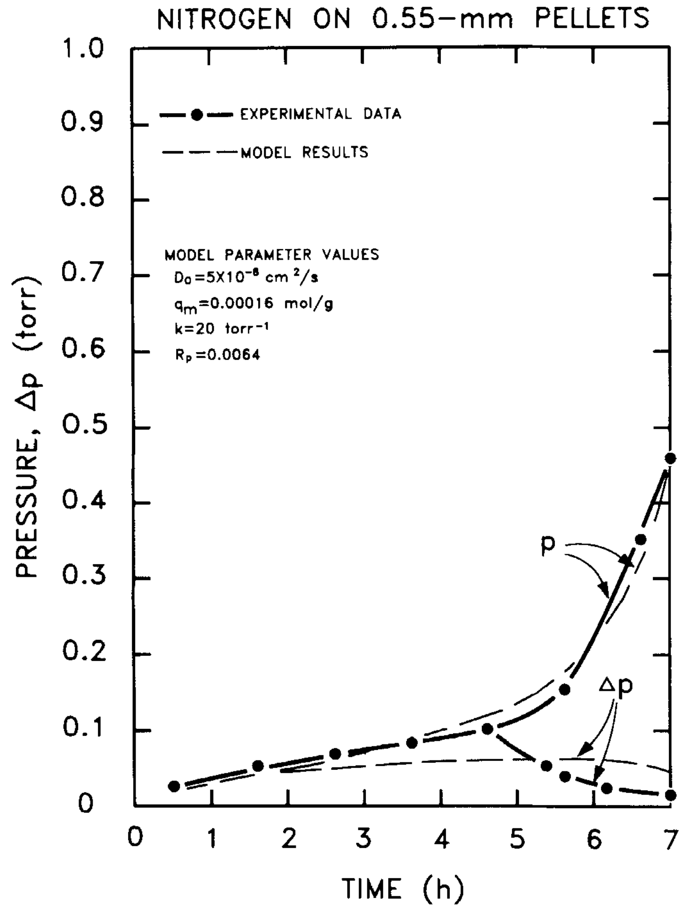

FIGURE 7. Comparison of experimental sorption pumping data for nitrogen on 0.55-mm spherical pellets of Davison 4A zeolite molecular sieves with the results of the proposed macropore-controlled model.

Table 2. BEST VALUES FOR MODEL PARAMETERS

	k(torr^{-1})	q_m (mmol/g)	r_p (cm)	D_0 (cm^2/s)
Argon (0.55 mm)	5	0.020	0.0005	5×10^{-8}
Argon (0.385 mm)	15	0.029	0.0003	5×10^{-8}
Oxygen (0.55 mm)	10	0.19	0.0007	5×10^{-8}
Oxygen (0.385 mm)	20	0.38	0.0003	5×10^{-8}
Nitrogen (0.55 mm)	20	0.16	0.0064	5×10^{-8}

Both Knudsen and molecular diffusivities are approximately proportional to (molecular weight)$^{-1/2}$, which would yield a macropore diffusivity variation of 20%, at most, for the three gases (O_2, Ar, and N_2). On this basis, the same macropore diffusivity of 5×10^{-8} cm^2/s was used for all gases. The pressure drop across the bed was very sensitive to the value of r_p, which characterizes the size of the interstitial voids in the bed. Matching the simulated results to the experimental results required values for r_p of 0.0003 cm for the beds of 0.385-mm pellets, and 0.0005 to 0.0007 cm for the beds of 0.55-mm pellets.

The data of Crabb et al. (6) for nitrogen were simulated reasonably well by the same procedure as those for argon and oxygen (Fig. 7). In this experiment, the flow rate of nitrogen was 3.0×10^{-8} mol/s, about 10 times the flow rate for the oxygen experiments. A summary of the parameter values that gave best agreement between the model and the experimental results for all three gases is given in Table 2.

CONCLUSIONS

The elucidation of the sorption behavior of the constituent pure gases of air has been completed for spherical Davison 4A molecular sieves in the course of this and the previously reported work (6). Previous work indicated that the vacuum sorption behavior of CO_2 at 193 K is micropore controlled. On the other hand, this study shows that there is clear evidence that diffusion in the pellets is macropore controlled for all of the other major gases in air (N_2, O_2 and Ar). It is possible that some sorption occurs on the clay binder, but more important is sorption in the surface layers of the crystals. This is shown by the different capacities of the sorbent for argon and oxygen. Considering the low equilibrium loadings and low extrapolated micropore diffusivities, penetration of the two species into the crystals must necessarily be quite low.

NOTATION

A	Cross-sectional area of bed, cm^2
$\overline{AG}$	Discretization matrix for gas, cm^{-1}
$\overline{AS}$	Discretization matrix for solid, cm^{-1}
c	Concentration of gas, mol/cm^3
c_i	Orthogonal polynomial coef. in trial solution,torr
d	Molecular diameter [in Eq. (10)], cm
d_i	Orthogonal polynomial coefficient in trial solution, mol/g molecular sieve
D	General diffusivity of sorbate in sorbent particle [Eq. (46)], cm^2/s
D_0	Corrected diffusivity, cm^2/s
D_K	Knudsen diffusivity, cm^2/s
D_M	Molecular diffusivity, cm^2/s
D_p	Pore diffusivity for bed, cm^2/s
D_{Pois}	Poiseuille diffusivity, cm^2/s
D_z	Zeolitic diffusivity, cm^2/s
k	Langmuir equilibrium constant, $torr^{-1}$
k_B	Boltzmann constant, J/K
L	Length of bed, cm
M	Number of interior collocation points in solid phase, or molecular weight of sorbate, mol/g
n	Number of moles in ideal gas equation
N	Number of interior collocation points in gas phase
p	Column pressure, torr
$\hat{p}$	Column pressure ratio, p/p_r
p_r	Reference pressure, torr
$\Delta p_{\max}$	Maximum pressure drop, torr
q	Point solid loading in sorbent particle, mol sorbed gas /g molecular sieve

$\bar{q}$	Average solid loading in sorbent particle, mol sorbed gas /g molecular sieve
$\hat{q}$	Solid loading, q/q_m
q_m	Langmuir saturation constant, mol/g molecular sieve
Q	Flow into headspace, torr·L/s
r	Radial position in sorbent particle, cm
$\hat{r}$	Radial distance ratio, r/R
r_p	Mean pore radius, cm
R	Sorbent particle radius, cm, or
R	Gas constant, torr·L/mol·K
t	Time, s
T_a	Ambient temperature, K
T	Bed and sorbate temperature, K
v	Gas velocity through bed, cm/s
V	Volume, cm^3
z	Axial distance along bed, cm
$\hat{z}$	Axial distance, z/L

Greek Letters

λ	Mean free path, cm
ϵ	Fraction of bed available to gas, cm^3 void/cm^3 bed
σ	Lennard-Jones collision diameter, m^{-10}
θ_z	Zeolite crystal surface area to volume ratio, cm^2/cm^3
θ_G	Fraction of bed available to gas, cm^3 void/cm^3 bed
ρ_b	Bulk density of molecular sieve, g/cm^3 bed
ϕ_Z	Sorbent fraction of bed volume, cm^3 sorbent /cm^3 bed
μ	Gas viscosity, g·cm/s
Ω	Lennard-Jones collision potential function

ACKNOWLEDGMENTS

The support of the Division of Chemical Sciences, Office of Basic Energy Sciences, U.S. Department of Energy under contract DE-AC05-84OR 21400 with Martin Marietta Energy Systems, Inc., is gratefully acknowledged. M. R. Gibson's efforts in the experimental program were invaluable.

REFERENCES

1. P. W. Fisher and J. S. Watson, Cryosorption Vacuum Pumping of Deuterium, Helium, and Hydrogen at 4.2 K for Controlled Thermonuclear Reaction Applications, Proceedings of the 24th Conference on Remote Systems Technology. (1976).
2. R. W. Dennison and G. R. Gray, J. Vac. Sci. Technol., 16, 2, (1979).

3. W. Wheeler, J. Vac. Sci. Technol., 11, 1, (1974).

4. K. S. Crabb and J. J. Perona, Mass Transfer in Vacuum Sorption Pumping of Pure Gases on Molecular Sieves, ORNL-6092, Oak Ridge National Laboratory, Oak Ridge, TN., (1985).

5. J. K. Prazniak and C. H. Byers 1987. A Modeling Study of Vacuum Sorption Characteristics of Carbon Dioxide on 4A Zeolite Molecular Sieves, ORNL/TM-10327, Oak Ridge National Laboratory, Oak Ridge, TN, (1987).

6. K. S. Crabb, J. J. Perona, C. H. Byers and J. S. Watson, AIChE J., 32, 255, (1986).

7. D. M. Ruthven, Principles of Adsorption and Adsorption Processes, Wiley, New York, (1984).

8. R. B. Bird, W. E. Stewart, and E. N. Lightfoot Transport Phenomena, Wiley, New York. (1960)

9. D. R. Garg and D. M. Ruthven, Chem. Eng. Sci., 28, 791, (1973).

10. D. M. Ruthven and R. I. Derrah, J. Chem. Soc. Farady Trans., 71, 2031, (1975).

11. D. M. Ruthven and R. I. Derrah, Can. J. Chem. Engr., 50, 743, (1972).